$\mathcal{R}$esearch in
$\mathcal{A}$stronomy and
$\mathcal{A}$strophysics

Location of energy source for coronal heating on the photosphere

Zhen-Xiang Hong[1,2], Xu Yang[3], Ya Wang[1,2], Kai-Fan Ji[4], Hai-Sheng Ji[2,3] and Wen-Da Cao[3,2]

[1] University of Chinese Academy of Sciences (CAS), Beijing 100049, China; *hongzx@pmo.ac.cn*

[2] Key Laboratory of DMSA, Purple Mountain Observatory, CAS, Nanjing 210008, China

[3] Big Bear Solar Observatory, NJIT, 40386 North Shore Dr, Big Bear City, CA 92314, USA

[4] Yunnan Observatories, CAS, Kunming 650011, China

Abstract It is reported that ultra-fine dynamic ejections along magnetic loops of an active region originate from intergranular lanes and they are associated with subsequent heating in the corona. As continuing work, we analyze the same set of data but focus on a quiet region and the overlying EUV/UV emission as observed by the Atmospheric Imaging Assembly (AIA) on board Solar Dynamics Observatory (SDO). We find that there appear to be dark patches scattered across the quiet region and the dark patches always stay along intergranular lanes. Over the dark patches, the average UV/EUV emission at 131, 171, 304 and 1600 Å (middle temperature) is more intense than that of other regions and EUV brightness is negatively correlated with 10830 Å intensity, though, such a trend does not exist for high temperature lines at 94, 193, 211 and 335 Å. For the same quiet region, where both TiO 7057 Å broad band images and 10830 Å filtergrams are available, contours for the darkest lane areas on TiO images and dark patches on 10830 Å filtergrams frequently differ in space. The results suggest that the dark patches do not simply reflect the areas with the darkest lanes but are associated with a kind of enhanced absorption (EA) at 10830 Å. A strict definition for EA with narrow band 10830 Å filtergrams is found to be difficult. In this paper, we define enhanced absorption patches (EAPs) of a quiet region as the areas where emission is less than ∼90% of the mean intensity of the region. The value is equivalent to the average intensity along thin dark loops connecting two moss regions of the active region. A more strict definition for EAPs, say 88%, gives even more intense UV/EUV emission over those in the middle temperature range. The results provide further observational evidence that energy for heating the upper solar atmosphere comes from the intergranular lane area where the magnetic field is constantly brought in by convection motion in granules.

Key words: Sun: atmosphere — Sun: photosphere — Sun: transition region — Sun: corona

1 INTRODUCTION

More than seven decades ago, solar physicists began to realize that the Sun's atmosphere exhibits a totally unexpected temperature distribution: its corona is much hotter than the underlying photosphere (which is regarded as the surface layer) (Grotrian 1939; Edlén 1943). The unusual temperature distribution has puzzled them ever since (Aschwanden 2004). Up to the present time, it is still not clear how radiation from the high temperature plasma in the corona is maintained. This is the prob-

lem of coronal heating, which many solar space missions and instrumentation of ground-based large-aperture solar telescopes have been specially designed to solve. A variety of mechanisms have been proposed; the two prevailing ones are dissipation of Alfvén waves (Hollweg 1981; De Pontieu et al. 2007a; McIntosh et al. 2011) and nanoflares (Parker 1983, 1988). To verify these models, the most important step is to identify the energy source (Klimchuk 2006). With a number of observational evidences, Aschwanden et al. (2007) pointed out that energy for heating the corona certainly comes from be-

low the corona. It is believed that heating processes are originally driven by constant photospheric motions, thus tracking down the energy source to the photosphere is fundamentally important. Despite the fact that extensive multi-wavelength observations of coronal heating have been made during the past years, direct evidence for heating events, which have been identified as originating from the photosphere, is still very rare. With data from the HINODE satellite and the Atmospheric Imaging Assembly on board the Solar Dynamics Observatory (SDO/AIA: Lemen et al. 2012), de Pontieu et al. (2007b) reported so-called "type II spicules," fairly small-scale, fast-moving jets observed as ubiquitous ejections of hot plasma from the chromosphere into the corona where they dissipate their energy. Relating spicules to coronal heating should be a major correct step toward understanding the physical connections between the corona and lower atmosphere, since it combines the coronal heating problem with the problem of the formation of the chromosphere, an expanse of partially ionized gas or plasma lying just above the solar surface (Judge & Casini 2012). In addition, observations are always ready to demonstrate there is a strong correlation between the brightness of the chromosphere and corona, showing that these two regions are powered by a similar mechanism (Schrijver & Zwaan 2000). However, we still do not know where and/or how these type II spicules are rooted in the solar surface.

We have seen that, to solve the problem of coronal heating, it is very important to have high-resolution observations of the solar interface region, which lies between the photosphere and the lower corona and plays a key role in obtaining physical links for all levels of the solar atmosphere. To acquire spectral and spatial information on the interface region is the key science goal of a recent NASA satellite called Interface Region Imaging Spectrograph (IRIS: De Pontieu et al. 2014a), aiming to obtain a comprehensive physical picture for energy flow in the upper solar atmosphere. To do this, IRIS has to collect spectral imaging from the chromosphere to the transition region, above which the chromosphere transforms into the even hotter corona. Recent high-resolution observations made by IRIS have provided fascinating new insights into the energetics of the lower solar atmosphere (e.g., De Pontieu et al. 2014b; Hansteen et al. 2014; Peter et al. 2014; Tian et al. 2014). Major findings include the discovery of prevalent small-scale jets, hot explosions and magnetic twisting on the Sun, which were found to be associated with injection of mass and energy into the

corona. Again, an exact pining down of these small-scale events to the photospheric layer has not been achieved.

With the advent of large aperture telescopes and advances in adaptive optics, narrow band He I 10830 Å imaging has proven to be an excellent choice for observing the interface region. The formation of the 10830 Å triplet requires extreme conditions which are mainly present in the upper solar chromosphere or lower corona. Except for flaring times, the triplet is optically thin, making the photosphere visible as background around the solar disk center (Judge et al. 2015). In this way, solar activity could be traced from the transition region or lower corona down to the photosphere with much less ambiguity. With the 1.6 m aperture New Solar Telescope at Big Bear Solar Observatory (BBSO/NST), Ji et al. (2012) (JCG hereafter), for the first time, obtained a new facet of the Sun's upper chromosphere using high resolution narrow band imaging at 10830 Å. The novel observations have proven to be very useful for resolving small-scale coronal heating events. For example, they were the first to report direct observations of dynamical events originating in the Sun's photosphere and subsequently lighting up the corona. However, as stated in their paper, more detailed statistics on ultrafine absorption features are needed. This is especially true for quiet regions and coronal holes. In this work, we use the same set of data but concentrate on a quiet region to pin down the enhanced 10830 Å absorption regions to the photosphere and find their relationship with emission from the overlying transition region as observed by SDO/AIA.

In Section 2 we give a short description of observations and data reduction. Results, and discussion and conclusion are presented in Section 3 and Section 4, respectively.

2 OBSERVATIONS AND DATA REDUCTION

The data analyzed in this research were obtained from the NST at BBSO on 2011 July 22 from 17:29:06 UT to 18:03:37 UT with the narrow band (bandpass 0.5 Å) at He I 10830 Å blue wing (–0.25 Å). It is the same set of data analyzed by JCG; for a detailed description of the observations, readers can refer to the corresponding paper. We used simultaneous space observations from SDO/AIA for information on hot plasma above the chromosphere. AIA was designed to study the response of the solar transition region or lower corona to characteristics of the Sun's dynamic magnetic field, by providing coverage of the full thermal range (Lemen et al.

2012). Since we want to investigate EUV emission by distinguishing intergranular lanes from granulations, the co-alignment between the NST 10830 Å and SDO/AIA images needs to be very precise. These co-alignments were carried out using NST TiO 7057 Å broad band images and Helioseismic and Magnetic Imager (HMI) (on board SDO) continuum images as the intermediaries. In 10830 Å narrow band filtergrams, the photosphere shines in as contaminating background. For high-resolution images, this background is packed with granulations, which give numerous features for an unprecedentedly precise co-alignment between chromosphere and photosphere images. We used common features such as sunspots and granulations to align these images. Figure 1 shows an example that demonstrates the alignment. Through repeated visual examination we believe that the accuracy of the co-alignment is much better than 0.5 arcsecond.

3 RESULTS

The left panel of Figure 2 shows a snapshot image (70 Mm × 70 Mm) taken with the He I 10830 Å narrow band Lyot filter. The field of view covers most of the active region NOAA 11259 on 2012 July 22. Below the coronal magnetic arcade of the active region, there appear especially narrow loops in absorption. These cooler and dark counterparts of higher lying EUV loops are highly dynamic, with material constantly flowing in and fading away. As mentioned previously, an He I 10830 Å narrow band image itself is an image with features from both the upper chromosphere and photosphere, thus the image represents a natural perfect co-alignment between the upper chromosphere and photosphere. This unique characteristic enabled JCG to report with confidence that the magnetic loops (in absorption) are actually rooted in intergranular lane areas. For a couple of dark ejections, they identified tempo-spatially correlated EUV brightening and concluded that the energy for heating these loops comes from an intergranular lane area, which is related to dynamics of magnetic flux concentrations.

Figure 3(a) displays a sample of a 10830 Å filtergram taken at 18:02:01 UT for the quiet region, the FOV of which is outlined by the red box in Figure 2. In addition, at this time, a nearby surge in absorption (Zeng et al. 2013) totally faded away, allowing us to have a larger FOV for a quiet region. Another reason is that we can have a TiO 7057 Å photosphere image with the same FOV for comparison, which is shown in panel (c). We can see that the 10830 Å filtergram bears a close re-

semblance with the photosphere due to the optically thin nature along the line of sight. Unlike a standard image of the photosphere, we can roughly see mist of a thin absorption layer, especially around intergranular lane areas. We see many dark regions, which are always located along intergranular lane areas. Some obvious ones are pointed out with white arrows in panel (a). We find that all noticeable dark regions in the 10830 Å filtergram can be outlined well with contours representing ∼90% of average band pass intensity for the quiet region (Fig. 3(b)). The ∼90% contour value is equivalent to the average intensity along thin dark loops connecting two moss regions of the active region. For comparison, the darkest areas of the intergranular lane in the TiO 7057 Å image are also selected with contours tracing ∼90% of the corresponding average intensity (blue ones in Fig. 3(d)). Note that Figure 3(d) is overlaid with the same contours (white) for 10830 Å darkenings as in Figure 3(b). We can see that contours outlining the darkest lane areas in the TiO 7057 Å image and EAPs in the 10830 Å filtergram are not associated either spatially or morphologically, i.e., the darkest lane areas do not necessarily overlap with the dark regions in the 10830 Å filtergram and vice versa. To be clearer, black arrows in panel (d) point to some of the darkest lane areas with little 10830 Å darkening and white arrows point to some 10830 Å dark regions with no darkest lane areas as background. We see that the dark regions could be enhanced absorption patches (EAPs) at 10830 Å even though there are some areas where they overlap each other.

In the following, we choose a rectangular quiet region contained in the white box shown in Figure 2 to investigate the evolution of UV/EUV emission over the EAPs. In selecting the quiet region, we have to avoid the region passing through the surge and remove an area of dead pixels, the position of which keeps shifting due to diurnal rotation of the FOV (they are represented by a white area in Fig. 1). Unfortunately, most of the region has exceeded the FOV of TiO images.

Figure 4 shows a time series of narrow band 10830 Å filtergrams for the region, overlaid with contours at 88% (red), 90% (green) and 95% (blue) of the mean intensity of each image. We again see that the possible EAPs are all situated along the intergranular lane areas and always stay away from granules. Their size and morphology change with time, being obviously associated with convection motion in the photosphere. To see spatial correlation of the EAPs with EUV emissions, the contours of these values at different times are overlaid on simulta-
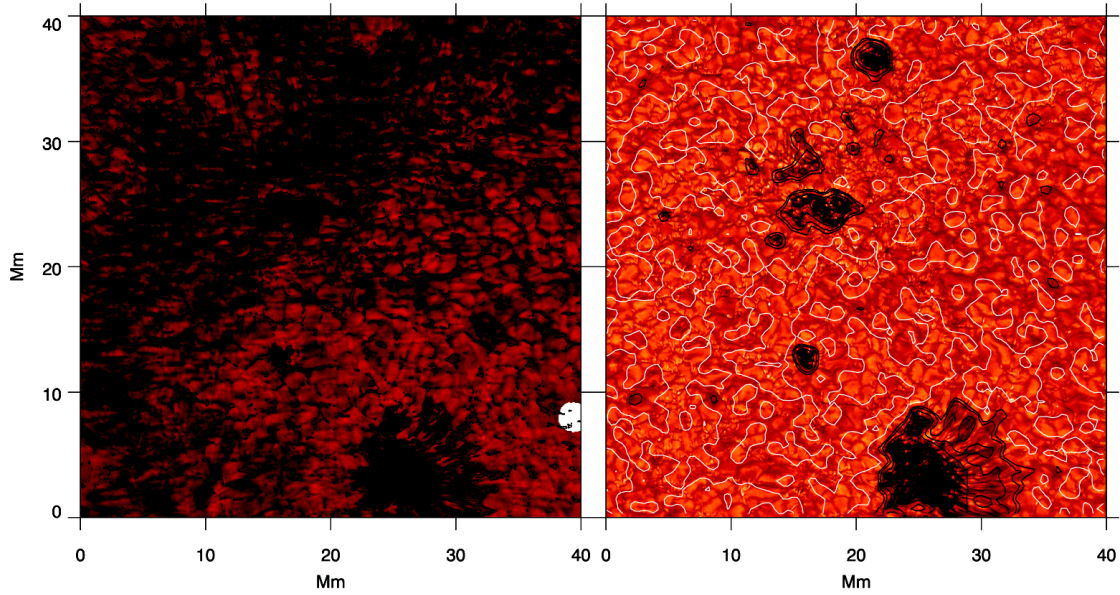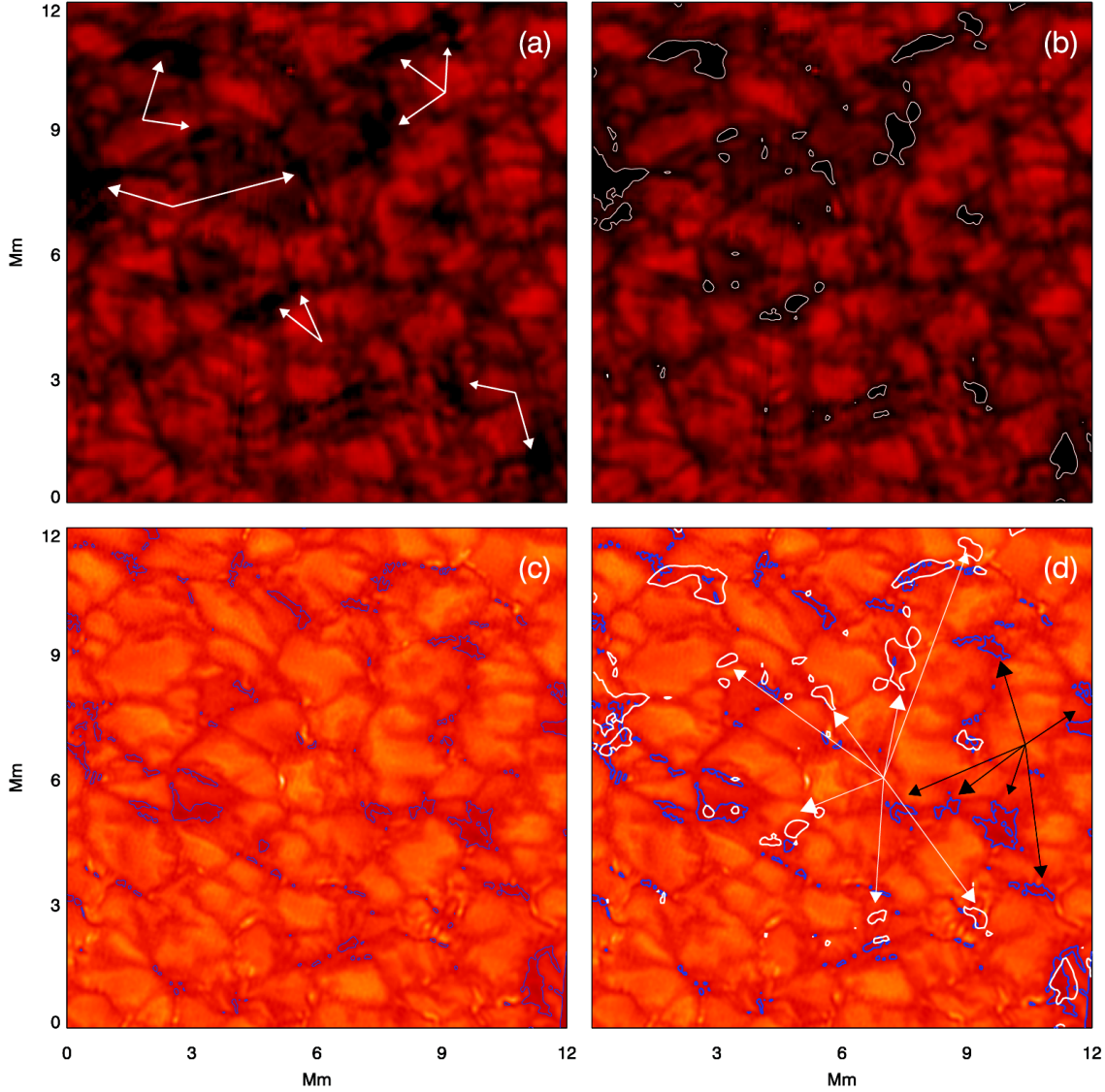
Fig. 1 An He I 10830 Å narrow band image (*left panel*) and a TiO 7057 Å broad band image (*right panel*) overlaid with contours representing intergranular lanes and sunspots from a simultaneous HMI continuum image. Note the *blank area* in the left panel which highlights where dead pixels were removed.
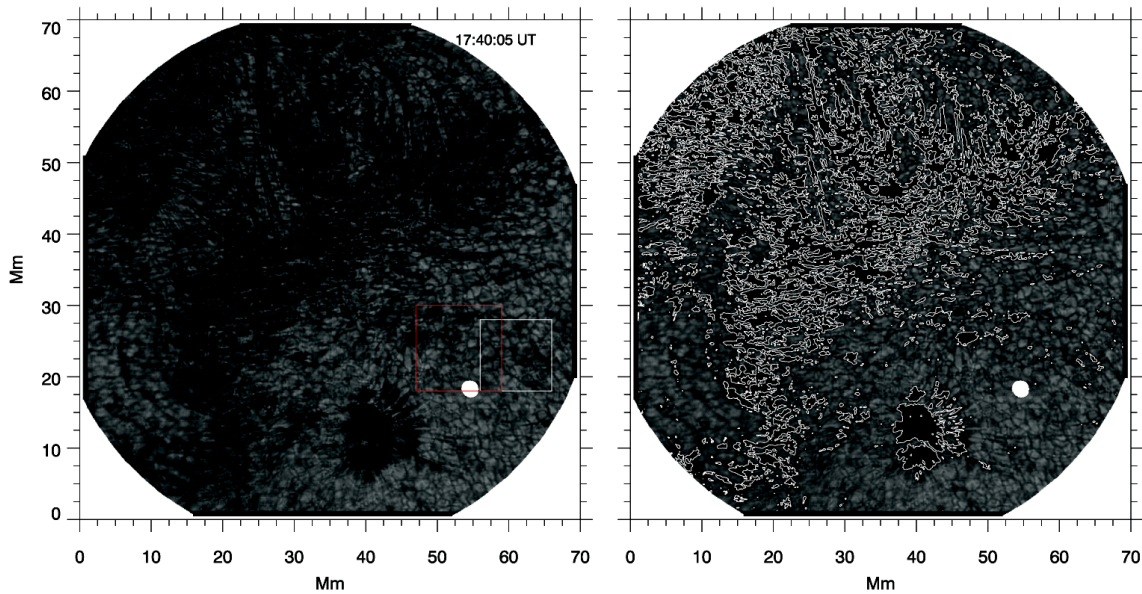
Fig. 2 *Left panel* shows an example snapshot of an He I 10830 Å narrow band image targeting the active region NOAA 11259 at 17:40:50 UT on 2012 July 22. The scale unit is Mm. The region in the white square is the selected quiet region being analyzed in this paper, while the region in the red square is the field of view for Fig. 3. The *right panel* shows the overlaid contours representing 90% of the mean intensity of the quiet region.

neous AIA 131 Å images in Figure 5. We get this result by rebinning AIA images, making them have the same pixel size as 10830 Å images. We see that 131 Å emission in the quiet region is not uniform at all, and bright emission looks like clouds against a relatively dark background. Most of the contours for 10830 Å EAPs are situated on bright emission regions, staying away from weak background. Now, we tentatively define regions which

Fig. 3 A comparison between darkening areas in an He I 10830 Å narrow band filtergram (a or b) and the darkest lane areas in a simultaneous (18:02:01 UT) TiO 7057 Å broad band image (c or d). *White arrows* in panel (a) point to 10830 Å darkening regions for visual inspection. Both kinds of images have the same field of view shown in Fig. 2. (b) The He I 10830 Å narrow band filtergram overlaid with contours (in white) representing 90% of the mean intensity of the region. (c) The TiO 7057 Å broad band image overlaid with (in *blue*) contours representing 90% of the mean intensity of the region at this band. (d) Same as panel (c), but additionally overlaid with contours (also in *white*) from panel (b). *White arrows* point to 10830 Å darkening regions with no darkest lane areas as background while *black arrows* point to darkest lane areas without obvious 10830 Å darkening.

have values below ∼90% of the mean intensity of quiet regions as 10830 Å EAPs.

Figure 6(a)–6(i) gives two kinds of time profiles of EUV/UV emissions: integrated over EAPs (red) and granules (black). We find that, at most times, EUV emissions at 131 Å, 171 Å, 304 Å and 1600 Å over the EAPs are more intense than those of other regions (panels 6(e), 6(f), 6(g) and 6(h)). This is true especially for the 131 and 1600 Å lines, for which emissions over the EAPs are always more intense. The magnitude of EUV/UV emission variation over EAPs is larger than the 5-σ value obtained from the time profile for the whole region. For the Sun's quiet region, the lines 131 Å, 171 Å, 304 Å and 1600 Å are sensitive to plasma with a temperature of $\log T$ at
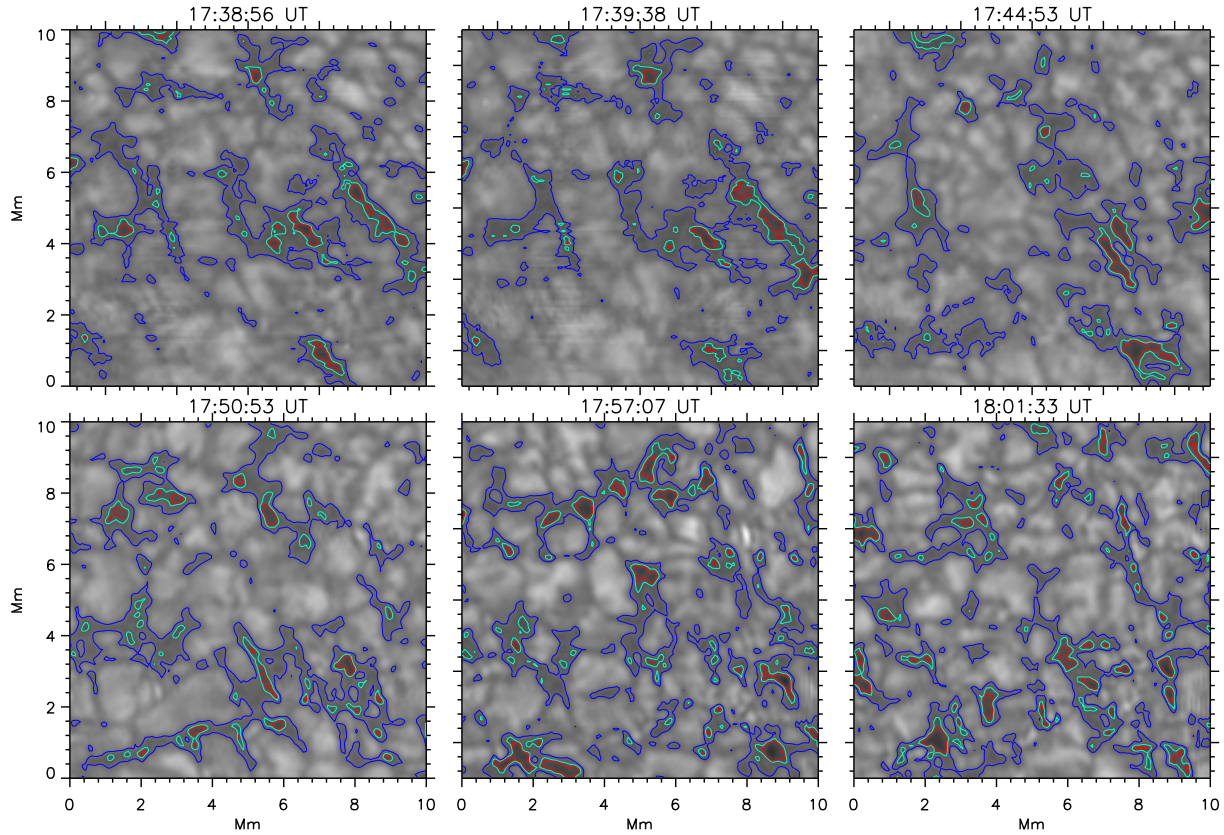
Fig. 4 A time series of narrow band 10830 Å filtergrams for the area outlined by the white box in Fig. 2, overlaid with contours at 88% (*red*), 90% (*green*) and 95% (*blue*) of the mean intensity in each image. An animation associated with this figure is available on line.

$\sim$5.6 (Fe VIII), $\sim$5.85 (Fe IX/X), $\sim$4.7 (He II) and 5.0 (C IV + continuum) respectively (O'Dwyer et al. 2010).

In this paper, we classify these lines as middle temperature lines ($5 \leq \log T \leq 6$). But for the lines 94 Å, 193 Å, 211 Å and 335 Å, such a trend vanishes. Their emission comes from plasma with higher temperature (high temperature lines in this paper), and these lines are especially selected for observation of flares and/or active regions. Although quiet regions also contribute to the emission of these lines, the contribution is all from million degree plasma (O'Dwyer et al. 2010). Note that the 94 Å emission falls into the noise level.

On the other hand, the emission of 1700 Å over EAPs exhibits an opposite variation trend when compared with that of middle temperature lines. Its emission has a negative correlation with hot plasma (Fig. 6(x)). AIA 1700 Å is expected to be able to observe the temperature minimum including the continuum from the photosphere with the temperature $\log T$ at $\sim$3.7 (low tempera-

ture). We speculate that the negative correlation may reflect the process of a local cool component being heated to hot plasma.

For the EAPs, there is a weak negative correlation between EUV brightness and 10830 Å absorption (Fig. 7). The correlation, by the way, may give support to the photo-ionization-recombination mechanism that populates Helium atoms to metastable levels (e.g., Avrett et al. 1994; Andretta & Jones 1997). We tried additional values of 88% and 95% as definitions of EAPs for analysis. A more strict definition for EAPs gives more intense EUV/UV emission in the middle temperature range compared to them.

The results for the AIA 131 Å emission are given in Figure 8, from which we can see that a more strict definition for EAPs of 88% gives even more intense 131 Å emission. In a similar way, the definition for EAPs by 95% gives weaker EUV emission. The results given in Figures 7 and 8 mutually support each other; both show
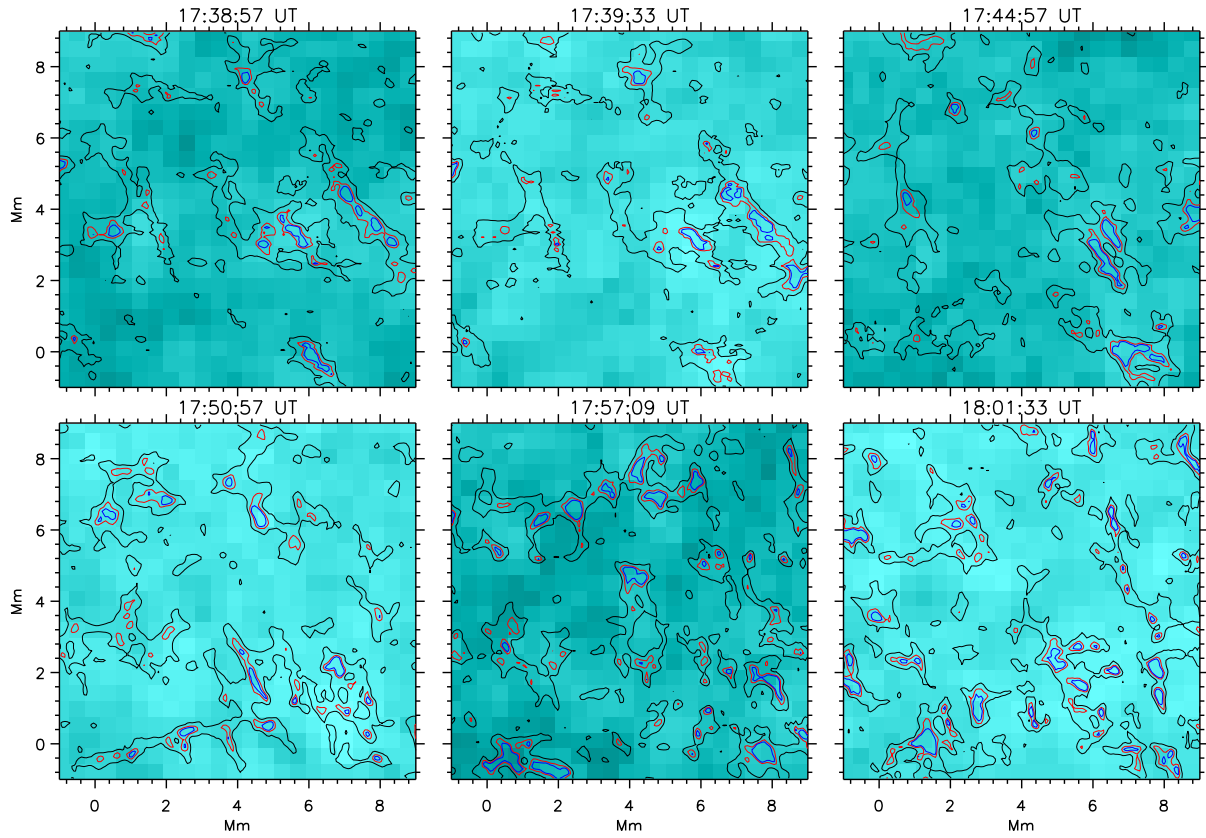
Fig. 5 A time series of AIA 131 Å images with the same field of view and overlaid with the same contours as Fig. 4. Note contour color has been changed for better visibility.
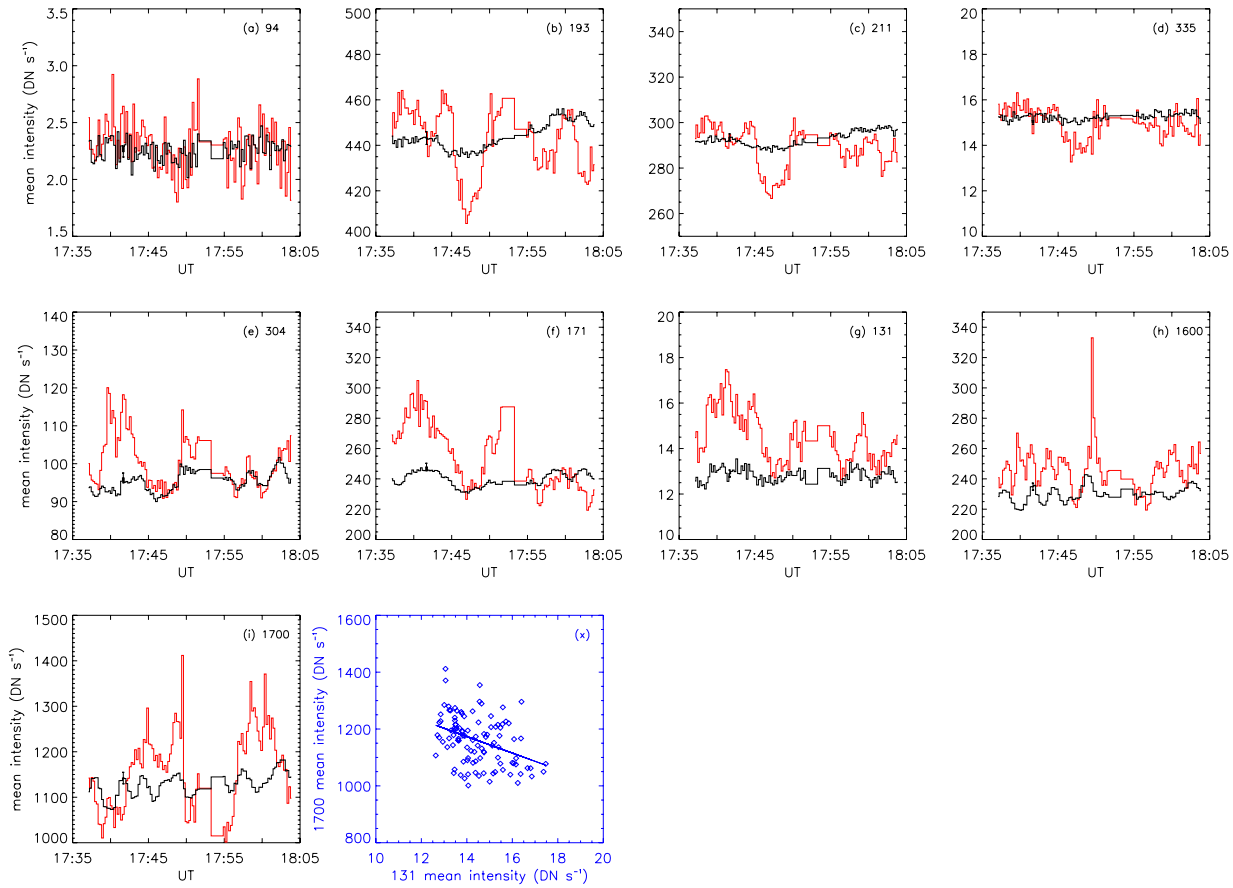
the correlation of enhanced 10830 Å absorption and simultaneous EUV/UV emission at middle temperature lines in some part of intergranular lane areas.

4 DISCUSSION AND CONCLUSION

More and more observational evidence has pointed out that the energy for heating the corona certainly comes from below the corona (Aschwanden et al. 2007). To make solid progress in solving the problem of coronal heating, it is most important to locate the energy sources on the photosphere. With high resolution and high cadence He I 10830 Å narrow band blue wing (–0.25 Å) images observed by the 1.6 m aperture NST at BBSO, we are motivated to pin down enhanced UV/EUV emissions on the photosphere via 10830 Å absorption features as intermediaries in the interface region. With this aim, we analyzed a quiet region, since it provides less ambiguity than a moss region, which is full of heavy spongy 10830 Å absorption features.

In this paper, the word "absorption" simply means a decrease in the counts over the instrument's narrow bandpass at 10830 Å, which can be affected by the following factors: line depth, like Doppler shift, width, core emission and background emission. Strictly speaking, for real 10830 Å absorption features, we need spectroscopic imaging, which will enable us to remove background emission. Considering the blue wing narrow band imaging for a quiet region, enhanced 10830 Å absorption can basically be caused by three factors: increased line depth, upward injection of material at the speed of $\sim 7 \, \mathrm{km \, s^{-1}}$ and a darker background. We have seen that 10830 Å dark features always stay along intergranular lane areas, therefore, one possibility is that they simply indicate the darkest lane areas. However, this possibility can be largely excluded due to the following reasons:

(1) The magnitude of the average intensity in the 10830 Å dark areas is equivalent to the emission along some thin magnetic loops of the active region, which are clearly observed as absorption.

Fig. 6 Panels (a–i): Time profiles of average EUV emission above the enhanced absorption regions (*red*) and other regions (*black*). Panel (x): 1700 Å intensity over EAPs versus that of 131 Å.
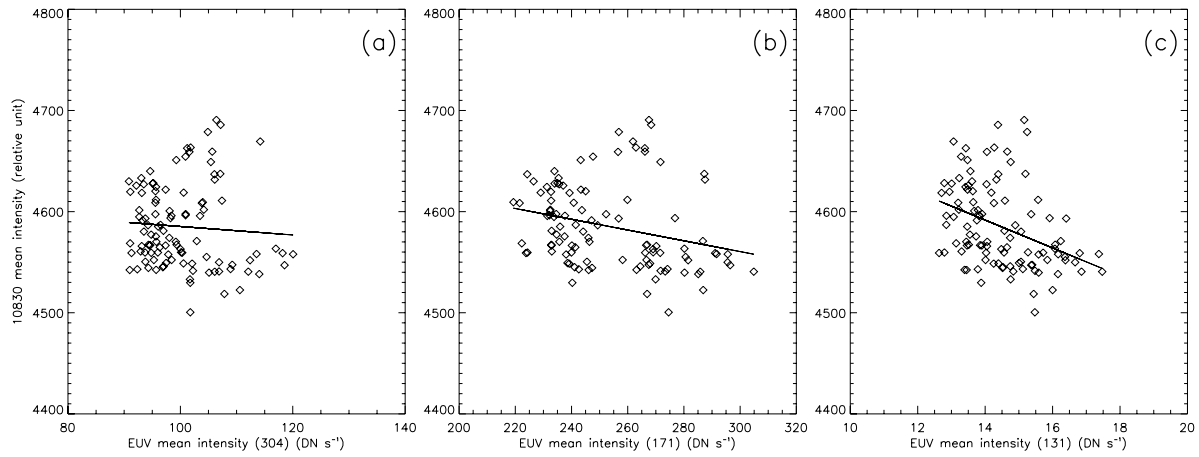
Fig. 7 The correlation between EUV emissions and 10830 Å intensity over the enhanced absorption regions.

(2) Detailed comparison results in Figure 3 show that the darkest lane areas in TiO 7057 Å images and in 10830 Å filtergrams are neither spatially nor morphologically associated.

(3) The darkest areas in 10830 Å filtergrams frequently accompany and maintain a similar morphology with bright EUV emissions (Fig. 5). This tendency persists, as Figure 6 indicates. That is, over the 10830 Å dark regions, average EUV/UV emission at 131,
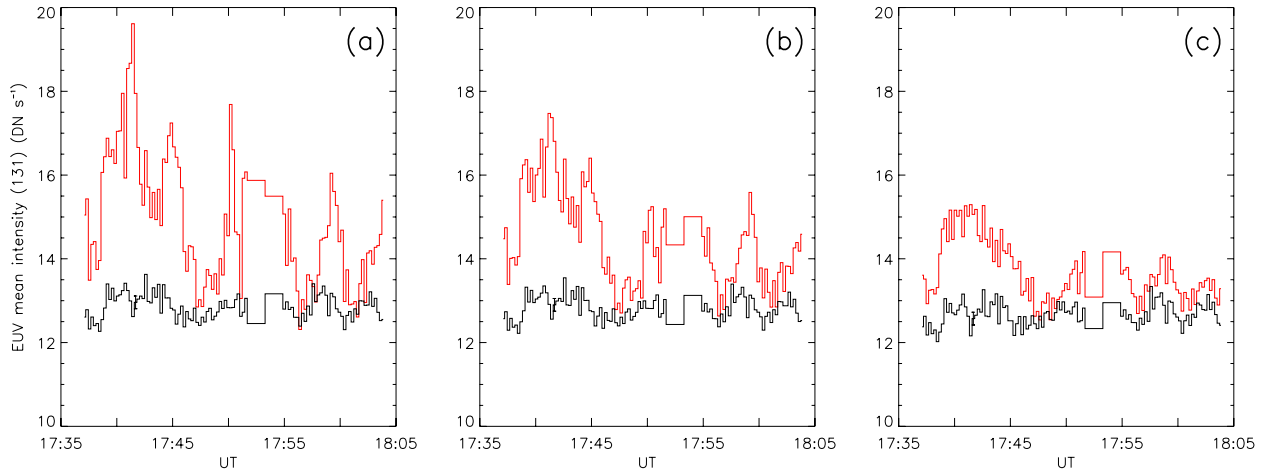
Fig. 8 *Red* profiles are for the time history of average 131 Å emission above the enhanced absorption areas which are defined as 88% (a), 90% (b) and 95% (c) of the mean intensity of each image. *Black* profiles are for the time history of average 131 Å emission of other corresponding areas.

171, 304 and 1600 Å lines (middle temperature) is more intense than that from other regions.

(4) A negative correlation exists between EUV brightness and 10830 Å intensity over the 10830 Å dark regions.

All the above results lead us to believe that, for the most part, the dark 10830 Å features along intergranular lane areas are EAPs. Remember that the observation was made at the blue wing (–0.25 Å), so the EAPs may reflect material flowing out from lane areas. In this regard, further investigations with high-resolution 10830 Å spectrograms taken by a Fabry-Perot interferometer at BBSO will further reveal the nature of EAPs.

For the first time, we try to pin down UV/EUV emissions in solar quiet regions on the photosphere with high-resolution observations. The results clearly show that energy for heating the Sun's upper atmosphere comes from intergranular lane areas, where small-scale magnetic activities are driven by constant granule convection. In other words, EUV emission over some intergranular lane areas serves as a driving component for the overall emission. This supports the discovery that there are two components of solar coronal emission made by EUV spectroscopic observations (Tian et al. 2011). This is only a preliminary work toward understanding the mysterious problem of coronal heating. More investigations, especially quantitative measurements, are necessary for a breakthrough. In this way, the source of high-speed solar wind could also be precisely located (Tian et al. 2010).

As a project in the near future, we will investigate some characteristics along intergranular lanes, like brightness, velocity and magnetic field, to find their relationship with overlying EUV/UV emission.

References

Andretta, V., & Jones, H. P. 1997, ApJ, 489, 375

Aschwanden, M. J. 2004, Physics of the Solar Corona. An Introduction (Praxis Publishing Ltd)

Aschwanden, M. J., Winebarger, A., Tsiklauri, D., & Peter, H. 2007, ApJ, 659, 1673

Avrett, E. H., Fontenla, J. M., & Loeser, R. 1994, in IAU Symposium, 154, Infrared Solar Physics, eds. D. M. Rabin, J. T. Jefferies, & C. Lindsey, 35

De Pontieu, B., McIntosh, S. W., Carlsson, M., et al. 2007a, Science, 318, 1574

de Pontieu, B., McIntosh, S., Hansteen, V. H., et al. 2007b, PASJ, 59, S655

De Pontieu, B., Title, A. M., Lemen, J. R., et al. 2014a, Sol. Phys., 289, 2733

De Pontieu, B., Rouppe van der Voort, L., McIntosh, S. W., et al. 2014b, Science, 346, 1255732

Edlén, B. 1943, ZAp, 22, 30

Grotrian, W. 1939, Naturwissenschaften, 27, 214

Hansteen, V., De Pontieu, B., Carlsson, M., et al. 2014, Science, 346, 1255757

Hollweg, J. V. 1981, Sol. Phys., 70, 25

Ji, H., Cao, W., & Goode, P. R. 2012, ApJ, 750, L25

Judge, P., & Casini, R. 2012, IAU Special Session, 6, E1.06

Judge, P. G., Kleint, L., & Sainz Dalda, A. 2015, ApJ, 814, 100

Klimchuk, J. A. 2006, Sol. Phys., 234, 41

Lemen, J. R., Title, A. M., Akin, D. J., et al. 2012, Sol. Phys., 275, 17

McIntosh, S. W., de Pontieu, B., Carlsson, M., et al. 2011, Nature, 475, 477

O'Dwyer, B., Del Zanna, G., Mason, H. E., Weber, M. A., & Tripathi, D. 2010, A&A, 521, A21

Parker, E. N. 1983, ApJ, 264, 642

Parker, E. N. 1988, ApJ, 330, 474

Peter, H., Tian, H., Curdt, W., et al. 2014, Science, 346, 1255726

Schrijver, C. J., & Zwaan, C. 2000, Solar and Stellar Magnetic Activity (Cambridge: Cambridge University Press)

Tian, H., Tu, C., Marsch, E., He, J., & Kamio, S. 2010, ApJ, 709, L88

Tian, H., McIntosh, S. W., De Pontieu, B., et al. 2011, ApJ, 738, 18

Tian, H., DeLuca, E. E., Cranmer, S. R., et al. 2014, Science, 346, 1255711

Zeng, Z., Cao, W., & Ji, H. 2013, ApJ, 769, L33